

## Original Research Article

# Dispersion modelling of carbon monoxide and total suspended particulate emission from cement stacks: case study of PT. Semen Tonasa in Indonesia

Fajar Septian Anwar<sup>1\*</sup>, Anwar Mallongi<sup>1</sup>, Alimin Maidin<sup>2</sup>

<sup>1</sup>Department of Environmental Health, <sup>2</sup>Department of Hospital Management, Faculty of Public Health, Hasanuddin University, Makassar, Indonesia

**Received:** 09 October 2018

**Accepted:** 26 October 2018

### \*Correspondence:

Mr. Fajar Septian Anwar,

E-mail: [fajarseptiananwar@gmail.com](mailto:fajarseptiananwar@gmail.com)

**Copyright:** © the author(s), publisher and licensee Medip Academy. This is an open-access article distributed under the terms of the Creative Commons Attribution Non-Commercial License, which permits unrestricted non-commercial use, distribution, and reproduction in any medium, provided the original work is properly cited.

## ABSTRACT

**Background:** Industrial activities in the cement production process produce emissions in the form of carbon monoxide (CO) and total suspended particulate (TSP) which have potential to cause environmental pollution in settlements around the industrial area. This study aimed to estimate the distribution emissions of CO and TSP concentrations at six settlements location around PT. Semen Tonasa of Pangkep Regency in a year.

**Methods:** This observational study was conducted by using descriptive approach. This study was conducted on May–June 2018. Meteorological data used for this study were air temperature, solar radiation, wind direction, and wind speed in 2014–2017 collected from Maros Climatology Station and data about seven main stack characteristics in 2014–2017 were collected from environmental services of South Sulawesi Province.

**Results:** The highest CO and TSP concentrations predicted in each location were respectively, 17.02  $\mu\text{g}/\text{m}^3$  and 6.56  $\mu\text{g}/\text{m}^3$  at Bontoa, 27.52  $\mu\text{g}/\text{m}^3$  and 10.4  $\mu\text{g}/\text{m}^3$  at Taraweang, 443.65  $\mu\text{g}/\text{m}^3$  and 148.41  $\mu\text{g}/\text{m}^3$  at Masjid Taqwa, 22.21  $\mu\text{g}/\text{m}^3$  and 3.1  $\mu\text{g}/\text{m}^3$  at Biringere, 1.17  $\mu\text{g}/\text{m}^3$  and 1.36  $\mu\text{g}/\text{m}^3$  at Kampung Sela, 19.07  $\mu\text{g}/\text{m}^3$  and at 15.54  $\mu\text{g}/\text{m}^3$  at Mangilu.

**Conclusions:** The dominant direction of CO and TSP dispersion was from the west. The highest concentrations were predicted at Masjid Taqwa in the most month. Maximum CO and TSP concentrations were not higher than the local regulation. Thus, it can be concluded that CO and TSP emissions from the cement plant have no impact on health in nearby communities.

**Keywords:** Cement industry, Dispersion modelling, CO, TSP

## INTRODUCTION

Air plays a very important role for the survival of human life and other living things, so that air is a natural resource that must be protected for the survival of life both now and in the future. To get air in accordance with the desired level of quality, air pollution control is very important to do. This is because air is an environmental medium that is very potential in the spread of diseases and chemicals that cause health problems. Changes in air quality are generally caused by air pollution, namely the

entry of pollutants (in the form of gases and small particles/aerosols) into the air.<sup>1</sup>

Air pollution is the cause of health problems that affect millions of people around the world based on statistical data released by the World Health Organization (WHO).<sup>2</sup> Contributors of air pollution come from natural sources and human activities, one of the contributors originating from human activities is industrial activity.<sup>3</sup> The cement industry is an industry with a high energy production process, because it requires a lot of fuel during the

combustion process in calcined and kilns. Emissions from the cement industry to the atmosphere include total suspended particulate (TSP), nitrogen oxides (NO<sub>x</sub>), sulfur oxides (SO<sub>x</sub>), carbon monoxide (CO), as well as minor pollutants such as semivolatile organic matter or heavy metals.<sup>4</sup>

CO gas can be harmful to human health. This CO gas will interfere with the binding of oxygen to the blood because CO is more easily bound by hemoglobin compared to oxygen and other gases.<sup>5</sup> TSP in ambient air has received serious attention because of its association with cardiovascular and respiratory.<sup>6</sup> Air quality greatly affects the ecology, environment, and health of people in an area. In recent years, several research efforts have been made to develop a prediction model for air quality. Atmospheric dispersion models are used to predict the concentration of air pollutants on the soil surface around the source.<sup>7</sup>

There are several reasons behind the importance of modeling air pollutants. First, the assessment of air pollution standards and measurement points is limited.

Furthermore, in all industrial areas, measurement and installation of assessment and monitoring stations are not feasible. Dispersion modeling uses mathematical equations, describes the atmosphere, the spread of chemicals to calculate concentrations in various locations. Gauss model analytically resolves the dominant equation, using the simplification of the premise.<sup>8</sup> If data for pollution sources and environmental conditions are adequate and easily accessible, air dispersion modeling has the potential to provide a more accurate assessment of possible exposure without requiring extensive monitoring.<sup>9</sup>

PT. Semen Tonasa is one of the largest cement plants in Eastern Indonesia which occupies a land area of 715 hectares in Biringere village, Bungoro district, Pangkep Regency. PT. Semen Tonasa was established in 1960 and now has four unit factories that can produce around six million tons of cement per year. People who lives around the cement plants are exposed to CO and TSP released into the atmosphere from the seven main stacks during the production processes. So, we have selected six settlements location around PT. Semen Tonasa of Pangkep for investigation (Figure 1).

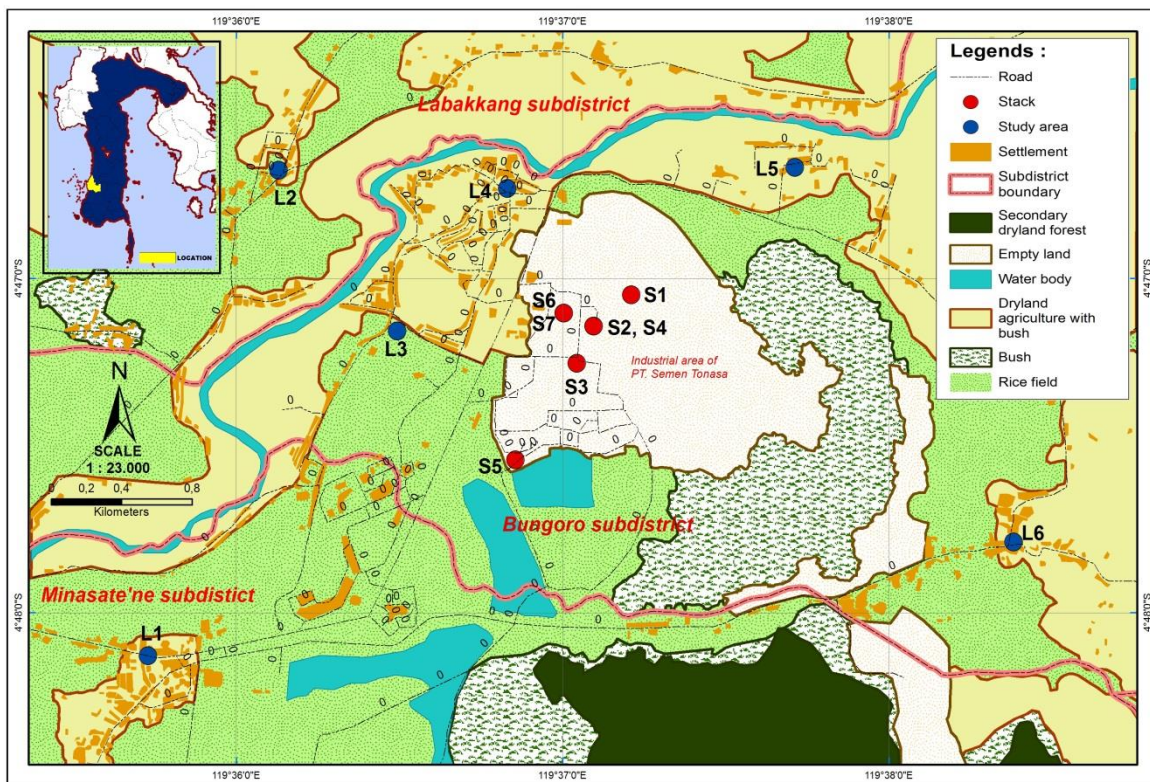


**Figure 1: Locations of the study areas.**

## METHODS

### Study design

This observational study was conducted by using Gauss model to estimate the distribution emissions of CO and TSP concentrations at six settlements location around PT. Semen Tonasa of Pangkep Regency in a year. This study

was conducted on May–June 2018. Meteorological data used for this study were air temperature, solar radiation, wind direction, and wind speed in 2014–2017 collected from Maros Climatology Station and data about seven main stack characteristics in 2014–2017 were collected from Environmental Services of South Sulawesi Province.

**Data analysis**

*WRPLOT view*

WRPLOT View – Freeware is a software that used to classifies the frequency of wind based on wind direction and speed to determine the distribution of eight wind directions, so that the main wind direction (dominant wind) will be obtained. The cumulative frequency of wind was used to made windrose diagrams during the measurement period (2014–2017).

*Gaussian dispersion models*

Calculation of concentrations at several receiving points is based on the emission level produced by each stack, then the concentration value at the same receiving point is accumulated. Calculation of pollutant concentrations using the Gaussian equation as follows:

$$C_{(x,y,z:H)} = \frac{Q}{2\pi U \sigma_y \sigma_z} \exp\left[-\frac{y^2}{2\sigma_y^2}\right] \left\{ \exp\left[-\frac{(z-H)^2}{2\sigma_z^2}\right] + \exp\left[-\frac{(z+H)^2}{2\sigma_z^2}\right] \right\} \quad [1]$$

where C is concentration of pollutants at coordinates x, y, z ( $\mu\text{g}/\text{m}^3$ ), Q is rate of emission of pollutants ( $\mu\text{g}/\text{sec}$ ), U is wind speeds in the stack height (m/sec),  $\sigma_y$  and  $\sigma_z$  are horizontal (cross wind) and vertical standard deviations of pollutant concentrations along the centre line of plume (i.e. dispersion coefficient) (m), x is downwind distance along the centre line of the plume (m), y and z are respectively, horizontal and vertical distance from the centre line of the plume ( $z=1$ , m), Also, H is effective plume height (m).<sup>10</sup>

**Table 1: Recommended power-law exponents for wind profile.**

Stability class	Rural exponent	Urban exponent
<b>A</b>	0.11	0.15
<b>B</b>	0.12	0.15
<b>C</b>	0.12	0.20
<b>D</b>	0.27	0.25
<b>E</b>	0.29	0.40
<b>F</b>	0.45	0.60

Source: Visscher, 2014.

**Table 2: Matrix for determining Pasquill-Gifford stability class.**

Wind speed (m/sec)	Daytime: Solar radiation			Nighttime: Cloud cover	
	Strong	Moderate	Slight	Cloudy	Clear
<2	A	B	B	E	F
2–3	B	B	C	E	F
3–5	B	C	C	D	E
5–6	C	C	D	D	D
>6	C	D	D	D	D

Source: Koehn et al., 2013.

Gaussian modeling can simply state particle deviations in the air over time. The amount of pollutants released regularly from the stack will be carried by the wind in the horizontal direction. Rate emission of pollutants (Q) can be calculated as:

$$Q = C \cdot A \cdot V \quad [2]$$

where C is concentration of pollutants at stack ( $\mu\text{g}/\text{m}^3$ ), A is stack cross-sectional area ( $\text{m}^2$ ), V is stack gas exit (m/sec).<sup>11</sup> For the calculation of wind speed in the stack height of cement plant, it is necessary to convert wind speed at 10 meters of ground-level as reference to wind speed in the stack nozzle of the source. The wind speed can be calculated as:

$$U = U_0 \left(\frac{Z}{Z_0}\right)^P \quad [3]$$

where U (m/sec) and  $U_0$  (m/sec) are the wind speeds in the stack height (Z, m) and observed wind speeds at 10 meters ( $Z_0$ , m), and P is the wind profile power-law exponents depending on the stability category (Table 1 and Table 2).<sup>12</sup> The downwind distance, x, and the horizontal distance, y, of a point source from a receptor are given by:

$$x = (S_p - S_r) \cos \theta + (R_p - R_r) \sin \theta \quad [4]$$

$$y = (S_p - S_r) \sin \theta - (R_p - R_r) \cos \theta \quad [5]$$

where  $R_p$ ,  $S_p$  are the coordinates of the point source;  $R_r$ ,  $S_r$  are the coordinates of the receptor, and  $\theta$  is the wind direction (the direction from which the wind blows). The units of x and y will be the same as those of the coordinate system R, S. Frequently a conversion is required in order to express x in kilometers and y in meters.<sup>13</sup>  $\sigma_y$  and  $\sigma_z$  represent the standard deviation of the Gauss distribution in the horizontal and vertical directions. Dispersion constant is not only a function of distance but also depends on atmospheric stability.<sup>14</sup> This dispersion constant is valid for use within 100 meters to 10 kilometers. Horizontal dispersion constant is expressed as:

$$\sigma_y = ax^b \quad [6]$$

The vertical dispersion constant is expressed as:

$$\sigma_z = cx^d + f \quad [7]$$

For coefficient value of a, c, d, and f were vary in each classification of atmospheric stability (Table 3).<sup>15</sup> Buoyancy flux ( $F_b$ ) calculated by using equation as follow:

$$F_b = \frac{g \cdot ws \cdot ds^2 \cdot (Ts-Ta)}{4 \cdot Ts} \quad [8]$$

where g is gravitational acceleration ( $9.8 \text{ m}/\text{sec}^2$ ), ws is velocity of gas flow (m/sec), ds is inside stack radius (m),



Ts and Ta are respectively, the initial plume temperature and the ambient temperature at the stack height (K).<sup>16</sup> For the calculation of rising buoyant plume ( $\Delta h$ ), the parameters of wind speed (U) and buoyancy flux ( $F_b$ ) are needed as following equation:

$$F_b < 55; \Delta h = \frac{21.45 F_b^{3/4}}{U} \quad [9]$$

$$F_b \geq 55; \Delta h = \frac{38.71 F_b^{3/5}}{U} \quad [10]$$

The final effective plume height (H in m) is calculated from the stack height (Z) and plume rise ( $\Delta h$ ) as follow:

$$H = Z + \Delta h \quad [11]$$

**Table 3: Coefficient value of a, b, c, d, and f for horizontal and vertical dispersion.**

Stability class	a	b	x ≤ 1 km			x > 1 km		
			c	d	f	c	d	f
A	213	0.894	440.8	1.941	9.27	459.7	2.094	-9.6
B	156	0.894	106.6	1.149	3.3	108.2	1.098	2.0
C	104	0.894	61.0	0.911	0	61.0	0.911	0
D	68	0.894	33.2	0.725	-1.7	44.5	0.516	-13.0
E	50.5	0.894	22.8	0.678	-1.3	55.4	0.305	-34.0
F	34	0.894	14.35	0.740	-0.35	62.6	0.180	-48.6

Source: Martin, 1976.

## RESULTS

The data in the form of stack characteristic in 2014–2017 and meteorological data in 2014–2017 were collected, then performed calculations by using a Gaussian dispersion model. The equations used to calculate the estimation of distribution emissions of CO and TSP concentrations at six settlements location around PT. Semen Tonasa of Pangkep Regency in a year.

The main emission source comes from the cement industry activity which was released through the seven main stacks with different characteristics each stack. The characteristics of each stack can be seen in Table 4. Table 4 shown that all stacks use coal as fuel and there were variations in the height and diameter of each stack. The other parameters which were stack temperature, stack gas exit, CO emission, and TSP emission, theirs value were the average value obtained from 2014 to 2017.

**Table 4: PT. Semen Tonasa main stack characteristics.**

Component	S1	S2	S3	S4	S5	S6	S7
Fuel	Coal	Coal	Coal	Coal	Coal	Coal	Coal
Stack height (m)	61.37	50.00	47.00	59.31	105.60	37.78	39.70
Stack diameter (m)	2.24	2.80	3.20	5.48	5.30	3.37	2.65
Stack temperature average (°C)	192.5	133	129.6	122	173.4	221	218
Stack gas exit average (m/sec)	22.34	15.02	11.65	23.50	27.04	20.35	51.78
Carbon monoxide emission average (mg/m <sup>3</sup> )	583	385.40	270.60	171.25	101.15	4.55	13.10
Total suspended particulate emission average (mg/m <sup>3</sup> )	66.12	63.99	59.40	62.26	46.07	68.03	70.42

**Table 5: Four-year air temperature average (°C).**

Month	Year				Average
	2014	2015	2016	2017	
January	25.87	26.27	27.72	26.48	26.59
February	26.69	26.51	27.11	26.70	26.76
March	26.94	26.78	27.62	26.81	27.04
April	27.23	27.18	27.99	27.36	27.44
May	27.78	27.73	28.41	27.57	27.87
June	27.58	26.79	27.49	26.75	27.15
July	26.91	26.76	26.83	26.80	26.83
August	26.64	26.87	27.47	27.58	27.14
September	27.32	28.01	28.12	28.32	27.94
October	28.88	29.03	27.53	27.85	28.32
November	28.09	28.70	27.59	27.17	27.89
December	27.07	27.19	27.29	27.10	27.16

**Table 6: Four-year solar radiation average (hours/day).**

Month	Year				Average
	2014	2015	2016	2017	
January	2.26	2.87	7.43	3.98	4.13
February	3.45	4.19	4.48	4.47	4.15
March	3.15	5.32	5.88	4.44	4.70
April	4.69	5.48	6.75	6.13	5.76
May	4.28	7.84	7.65	6.13	6.47
June	3.31	6.62	6.80	4.70	5.36
July	5.41	10.57	7.68	5.91	7.39
August	6.17	10.87	9.57	7.96	8.65
September	8.62	10.56	7.35	8.48	8.75
October	7.69	8.55	5.91	7.62	7.44
November	5.22	7.93	5.94	6.09	6.29
December	3.50	5.28	5.10	4.41	4.57

**Table 7: Stack distance to settlements location around PT. Semen Tonasa, Pangkep regency.**

Location code	Location	Coordinate point (S/E)	Stack distance to location (meter)						
			S1	S2	S3	S4	S5	S6	S7
L1	Bontoa	4°48'7.70" 119°35'43.70"	3402	3127	2931	3127	2357	3035	3035
L2	Taraweang	4°46'40.50" 119°36'7.70"	2123	1992	2008	1992	2098	1807	1807
L3	Masjid Taqwa	4°47'8.40" 119°36'29.40"	1347	1122	1048	1122	1007	955	955
L4	Biringere	4°46'43.80" 119°36'49.80"	920	908	1049	908	1507	764	764
L5	Kampung Sela	4°46'40.00" 119°37'42.70"	1170	1444	1650	1444	2272	1544	1544
L6	Mangilu	4°47'47.30" 119°38'22.90"	2571	2672	2674	2672	2869	2856	2856

\*S1 (Limestone Dryer II), S2 (Kiln II), S3 (Kiln III), S4 (Kiln IV), S5 (Kiln V), S6 (Grate Cooler IV), S7 (Grate Cooler V).

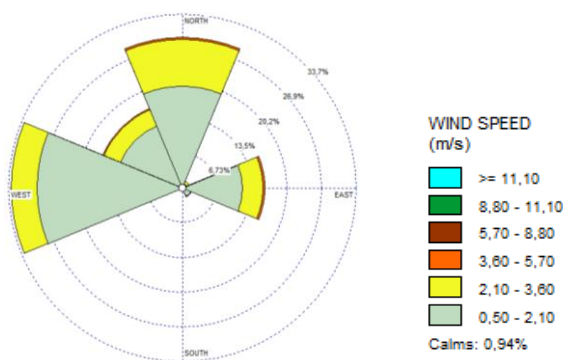


**Figure 2: Four-year windrose diagram of wind direction and speed.**

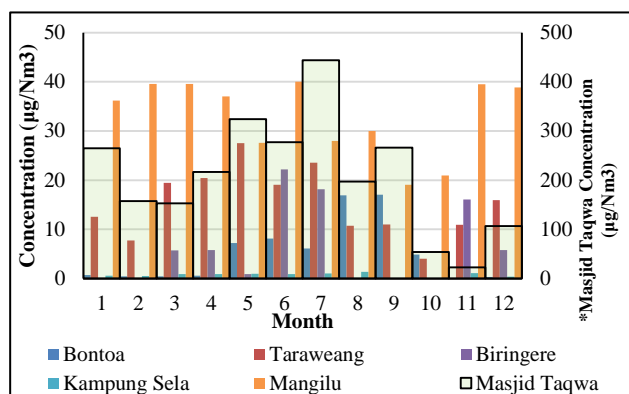
Table 5 shown that the highest air temperature was in October ranged from 27.53°C to 29.03°C and the lowest air temperature was in January ranged from 25.87°C to 27.72°C. Table 6 shown that the highest solar radiation was in September ranged from 7.35 hours/day to 10.56 hours/day and the lowest solar radiation was in January ranged from 2.26 hours/day to 7.43 hours/day.

Figure 2 shown the four-year windrose diagram of wind direction and speed. The majority of the wind direction moves from west with a frequency of 32.99% and an average speed of 1.35 m/sec, then followed by wind direction that moves from north with a frequency of 29.09% and an average speed of 1.48 m/sec.

Figure 3 shown that the distribution pattern of CO concentrations varies every month at each location. At Bontoa, the highest CO concentrations was 17.02 µg/m<sup>3</sup> in September and was not found at all (0 µg/m<sup>3</sup>) in November. At Taraweang, the highest CO concentrations was 27.52 µg/m<sup>3</sup> in May and the lowest was 4.05 µg/m<sup>3</sup> in October. At Masjid Taqwa, the highest CO concentrations was 443.65 µg/m<sup>3</sup> in July and the lowest was 23.04 µg/m<sup>3</sup> in November.

Furthermore, at Biringere, the highest CO concentrations was 22.21 µg/m<sup>3</sup> in June and was not found at all (0 µg/m<sup>3</sup>) in January, February, August, September and October. At Kampung Sela, the highest CO concentrations was 1.17 µg/m<sup>3</sup> in August and was not found at all (0 µg/m<sup>3</sup>) in September and October. At

Mangilu, the highest CO concentrations was  $40 \mu\text{g}/\text{m}^3$  in June and the lowest was  $19.07 \mu\text{g}/\text{m}^3$  in September.



**Figure 3: Estimation of the distribution pattern of CO concentration at settlements location in a year.**

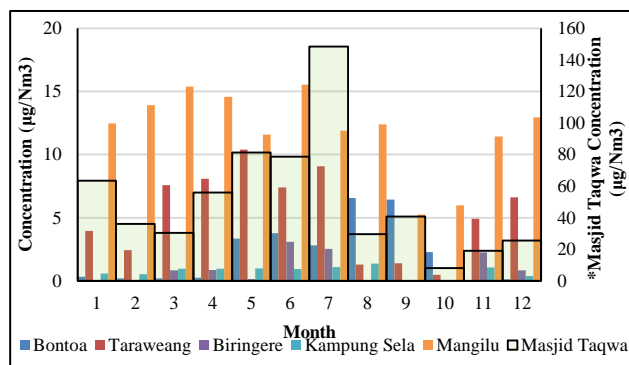


**Figure 4: Estimation of the distribution pattern of TSP concentration at settlements location in a year.**

Figure 4 shown that the distribution patterns of TSP concentrations varies every month at each location. At Bontoa, the highest TSP concentrations was  $6.56 \mu\text{g}/\text{m}^3$  in August and was not found at all ( $0 \mu\text{g}/\text{m}^3$ ) in November. At Taraweang, the highest TSP concentrations was  $10.4 \mu\text{g}/\text{m}^3$  in May and the lowest was  $0.48 \mu\text{g}/\text{m}^3$  in October. At Masjid Taqwa, the highest TSP concentrations was  $148.41 \mu\text{g}/\text{m}^3$  in July and the lowest was  $8.04 \mu\text{g}/\text{m}^3$  in October.

Futhermore, at Biringere, the highest TSP concentrations was  $3.1 \mu\text{g}/\text{m}^3$  in June and was not found at all ( $0 \mu\text{g}/\text{m}^3$ ) in January, February, August, September and October. At Kampung Sela, the highest TSP concentrations was  $1.36 \mu\text{g}/\text{m}^3$  in August and was not found at all ( $0 \mu\text{g}/\text{m}^3$ ) in September and October. At Mangilu, the highest TSP concentrations was  $15.54 \mu\text{g}/\text{m}^3$  in June and the lowest was  $5.25 \mu\text{g}/\text{m}^3$  in September.

**DISCUSSION**

The Gaussian model is one of the mathematical models used to present the process of gas pollutant dispersion in the air.<sup>17</sup> This model is based on the assumption that

plume are dispersed, and pollutants are dispersed in them, resulting from molecular diffusion, and because of diffusion, pollutant concentrations in both dimensions horizontally and vertically distributed normally (bell shaped curve). The shape of the plume, as well as the values of pollutant concentrations, vary in response to different atmospheric meteorological conditions.<sup>18</sup> The equation of the model is also used to determine the concentration of pollutants produced by industry stacks on specific locations around the plant.<sup>19</sup>

Based on the results that shown in Figure 3 and Figure 4, the estimation of CO and TSP concentrations at six settlements location around the PT. Semen Tonasa does not exceed the specified quality standard of 24-hour air quality measurement which are  $10,000 \mu\text{g}/\text{Nm}^3$  for CO and  $230 \mu\text{g}/\text{Nm}^3$  for TSP. Standard that used was Regulation of the South Sulawesi Governor Number 69 in 2010 about Quality Standards and Environmental Damage Criteria.

CO and TSP concentrations tend to be higher in the dry season (April–September) than in the rainy season (October–March). This was due to local meteorological factors which include air temperature, solar radiation, wind direction, and wind speed. In addition to meteorological factors, emission sources also influenced which were stack height, stack diameter, stack temperature, stack gas exit, stack distance to the location, and also CO and TSP emissions that produced by each stack (Table 6 and Table 7).

High air temperature makes the density of air near the surface of the earth to be lower than the air above it causing an upward flow of convection carrying various pollutants. This can cause pollutant concentrations to be low. Low air temperature causes the density of air near the earth's surface to be almost the same as the air density above it, as a result the air convection flow moves more slowly so that the pollutant concentrations becomes high because it accumulates on the surface.<sup>20</sup> Similar result study in London shown that particle number count was minimum in August, and a winter maximum, apparently in an inverse relationship with atmospheric temperature.<sup>21</sup>

Solar radiation can also measured in hours/day, that is the length of the sun shines on the earth in a period of one day. The one-day period is also called the length of the day, which is the length of the sun at the horizon. Changes in the length of the day are not so great in the Tropics area that are close to the equator. The farther location to the equator, the greater the fluctuation of the irradiation time.<sup>22</sup>

Solar radiation and wind speed greatly affect atmospheric stability which generally fluctuates. Both of these factors give rise to variations in air pressure between the layers of air near the surface of the soil with a higher layer of air. When the difference in air pressure between the two

layers is large, as often happens during the day, the atmosphere becomes unstable. Because there is no solar radiation, variations in air pressure at night are generally not too large. This causes the atmosphere to have a more stable condition at night.<sup>23</sup>

Pollutants in the air spread horizontally and vertically due to wind direction and speed. Large wind speeds can cause pollutants to experience large dilutions. The concentration of air pollutants from point sources is more sensitive to wind direction than other parameters. Seasonal factors can cause wind direction variations to be 360°.<sup>23</sup>

Wind speed is affected by horizontal pressure and temperature gradient (the higher the pressure gradient, the higher the wind speed) and the wind speed affects the travel time from the source to the receptor, halving the wind speed will double the travel time.<sup>18</sup> Wind direction and speed are the main components in making windrose diagram. Windrose diagrams are used as meteorological information related to the dispersion of pollutants, which illustrates changes in wind direction and speed in a diagram at a given time and region.<sup>24</sup>

The results also showed that CO and TSP concentrations were high at Masjid Taqwa for most of the month, this was due to the location distance close to the emission sources (955 to 1345 meters) and supported by unstable atmospheric condition and the wind direction that blew to the location. Similar result study in Iran shown that the worst condition occurred in spring in an unstable condition in which the maximum concentration of pollutant measured near the cement plant was at a higher level than in the other seasons.<sup>25</sup>

CO and TSP have harmful effects on human health. When inspired, environmental CO diffuses rapidly across the alveolar capillary membrane and binds to hemoglobin, forming carboxyhemoglobin (COHb). The affinity of hemoglobin for CO is 240 times greater than that for oxygen. High levels of COHb interfere with oxygen binding to and dissociation from hemoglobin resulting in impaired tissue oxygen delivery. Thus, overt CO toxicity results from tissue hypoxia and signs and symptoms appear when COHb is greater than 10%. The infant and fetus are more susceptible to CO toxicity than adults due to higher rates of metabolism and the presence of fetal hemoglobin, which has a greater affinity for CO than adult hemoglobin.<sup>26</sup>

Exposure to particulate has been identified as the cause of numerous health effects including increased hospital admissions, emergency room visits, respiratory symptoms, exacerbation of chronic respiratory and cardiovascular diseases, decreased lung function, and premature mortality. Particles that have the most impact on human health effects have been acknowledged to be those less than 10 µm in diameter. These particles can

penetrate within the respiratory tract beginning with the nasal passages to the alveoli, deep within the lungs due to their excessive penetrability. These particles can affect gas exchange within the lungs and can even penetrate the lung.<sup>27</sup> Particles smaller than 1 µm in general behave similar to gas molecules and will therefore penetrate down to the alveoli (deposition by diffusion forces), and can translocate further into the cell tissue and/or circulation system.<sup>28</sup> Similar result study in Indonesia shown that there was a significant relationship between particulate exposure and the incidence of respiratory disorders in the community in Kairagi Satu Lingkungan Tiga of Manado City.<sup>29</sup>

## CONCLUSION

The results of this study showed that the Gauss model is one of the models used for estimating air pollutant distribution. The dominant direction of CO and TSP dispersion was from the west. The highest concentrations were predicted at Masjid Taqwa in the most month. Maximum CO and TSP concentrations were not higher than the local regulation. Thus, it can be concluded that CO and TSP emissions from the cement plant have no impact on health in nearby communities.

## ACKNOWLEDGEMENTS

This study received funding from Indonesia Endowment Fund for Education (LPDP), Ministry of Finance, Indonesia.

*Funding: Funding from Indonesia Endowment Fund for Education (LPDP), Ministry of Finance, Indonesia*

*Conflict of interest: None declared*

*Ethical approval: Not required*

## REFERENCES

1. Mallongi, A. Bahan pencemar toxic di udara dan upaya pengendaliannya. Makassar: Penerbit WR; 2015.
2. Aggarwal P, Jain S. Impact of air pollutants from surface transport sources on human health: A modeling and epidemiological approach. *Environ Int.* 2015;83:146-57.
3. Borrego C, Coutinho M, Costa AM, Ginja J. Challenges for a new air quality directive: The role of monitoring and modelling techniques. *Urban Climate.* 2015;14:328-41.
4. Schuhmacher, M., M. Nadal, and J.L. Domingo. Environmental monitoring of PCDD/Fs and metals in the vicinity of a cement plant after using sewage sludge as a secondary fuel. *Chemosphere.* 2009;74(11):1502-8.
5. Luttrell WE, Jederberg WW, Still KR. *Toxicology principles for the industrial hygienist.* Virginia: AIHA; 2008.
6. Nkhama E, Ndhlovu M, Dvonch JT, Lynam M, Mentz G, Siziya S, et al. Effects of airborne

- particulate matter on respiratory health in a community near a cement factory in Chilanga, Zambia: Results from a panel study. *Int J Environ Res Public Health.* 2017;14(11):1351.
7. Singh KP, Gupta S, Kumar A, Shukla SP. Linear and nonlinear modeling approaches for urban air quality prediction. *Sci Total Environ.* 2012;426:244-55.
  8. Noorpoor A, Rahman H. Application of AERMOD to local scale diffusion and dispersion modeling of air pollutants from cement factory stacks (Case study: Abyeck cement factory). *Pollution.* 2015;1(4):417-26.
  9. Maroko AR. Using air dispersion modeling and proximity analysis to assess chronic exposure to fine particulate matter and environmental justice in New York City. *Applied Geography.* 2012;34:533-47.
  10. Arya SP. Air pollution meteorology and dispersion. Vol. 310. Oxford University Press New York; 1999.
  11. EPA U. User's guide for the Industrial Source Complex (ISC3) dispersion models. Description of Model Algorithms, vol. IIU. S. Environmental Protection Agency. Office of Air Quality Planning and Standards. Emissions, Monitoring, and Analysis Division, Research Triangle Park, North Carolina. 1995.
  12. Koehn AC, Leytem AB, Bjerneberg DL. Comparison of atmospheric stability methods for calculating ammonia and methane emission rates with windtrax. *Transactions of The ASABE.* 2013;56(2):763-8.
  13. Novak JH, Turner DB. An efficient Gaussian-plume multiple-source air quality algorithm. *Journal of the Air Pollution Control Association.* 1976;26(6):570-5.
  14. Tiwary A, Williams I. Air pollution: Measurement, modelling and mitigation. Boca Raton: CRC Press; 2018.
  15. Martin AD. Dispersion relation constraints on low energy KN scattering. *Physics Letters B.* 1976;65(4):346-50.
  16. Visscher A. Air dispersion modelling. New Jersey: John Wiley & Sons; 2014.
  17. Assomadi AF, Widodo B, Hermana J. The kinetic approach of NO<sub>x</sub> photoreaction related to ground measurement of solar radiation in estimates of surface ozone concentration. *Int J Chem Tech Res.* 2016;9(7):182-90.
  18. Vallero, D. Fundamentals of air pollution. London: Academic Press; 2014.
  19. Dewi NWSP. Estimasi pola dispersi debu, SO<sub>2</sub> dan NO<sub>x</sub> dari PT Holcim Indonesia Tbk, Bogor menggunakan model Gauss. *Jurnal Pengelolaan Sumberdaya Alam dan Lingkungan.* 2018;8(1):109-19.
  20. Syech, R. Faktor-faktor fisis yang mempengaruhi akumulasi nitrogen monoksida dan nitrogen dioksida di udara pekanbaru. *Komunikasi Fisika Indonesia.* 2014;10(7):516-23.
  21. Bigi A, Harrison RM. Analysis of the air pollution climate at a central urban background site. *Atmospheric Environ.* 2010;44(16):2004-12.
  22. Hamdi S. Mengenal lama penyinaran matahari sebagai salah satu parameter klimatologi. *Berita Dirgantara.* 2014;15(1):7-15.
  23. Godish T, Davis WT, Fu JS. Air quality. Boca Raton: CRC Press; 2014.
  24. Magidi S. Determining The Atmospheric Stability Classes for Mazoe in Northern Zimbabwe. *Int J Engineering Res Applications.* 2013;3(2):178-81.
  25. Goudarzi G, Rashidi R, Keishams F, Moradi M, Sadeghi S, Masihpour F, et al. An assessment on dispersion of carbon monoxide from a cement factory. *Environ Health Engineering Management J.* 2017;4(3):163-8.
  26. Levy RJ. Carbon monoxide pollution and neurodevelopment: A public health concern. *Neurotoxicol Teratol.* 2015;49:31-40.
  27. Fu M, Zheng F, Xu X, Niu L. Advances of study on monitoring and evaluation of PM<sub>2.5</sub> pollution. *Meteorol Disaster Reduction Res.* 2011;34:1-6.
  28. Kim KH, Kabir E, Kabir S. A review on the human health impact of airborne particulate matter. *Environ Int.* 2015;74:136-43.
  29. Thaib YP, Lampus B, Akili R. Hubungan antara paparan debu dengan kejadian gangguan saluran pernafasan pada masyarakat Kelurahan Kairagi Satu Lingkungan Tiga Kota Manado. *Jurnal Administrasi Publik.* 2015;4(32).

**Cite this article as:** Anwar FS, Mallongi A, Maidin A. Dispersion modelling of carbon monoxide and total suspended particulate emission from cement stacks: case study of PT. Semen Tonasa in Indonesia. *Int J Sci Rep* 2018;4(11):266-73.